

LTH823  
HU-EP-09/09  
SFB/PPP-09-23

# The $\omega$ - $\rho$ meson mass splitting and mixing from lattice QCD.



C. McNeile<sup>(a)</sup>, C. Michael<sup>(b)</sup>, C. Urbach<sup>(c)</sup>

- <sup>(a)</sup> Department of Physics and Astronomy, The Kelvin Building,  
University of Glasgow, Glasgow G12 8QQ, UK
- <sup>(b)</sup> Theoretical Physics Division, Dept. of Mathematical Sciences,  
University of Liverpool, Liverpool L69 7ZL, UK
- <sup>(c)</sup> Institut für Elementarteilchenphysik, Fachbereich Physik,  
Humbolt Universität zu Berlin, D-12489, Berlin, Germany

## Abstract

---

We compare flavour singlet and non-singlet vector mesons from first principles using lattice QCD. With  $N_f = 2$  flavours of light quark, this addresses the  $\omega$ - $\rho$  mass difference. Using maximally twisted-mass lattice QCD, we are able for the first time to determine this mass difference precisely and we compare with experiment. We also discuss  $\omega$ - $\rho$  mixing effects arising within QCD through the  $u$ - $d$  quark mass difference.

---

# 1 Introduction

The vector mesons are well described by a quark model since they are approximately ‘ideally’ mixed, with the flavour non-singlet ( $\rho$ ) and flavour singlet ( $\omega$ ) degenerate. Experimentally [1] the  $\omega$ - $\rho$  mass splitting is small (7 MeV). This is in contrast to the pseudoscalar mesons where the  $\eta$  and  $\eta'$  are much heavier than the  $\pi$ . From first principles in QCD, this splitting of flavour singlet and non-singlet meson occurs because of contributions from disconnected quark diagrams. These disconnected contributions can be evaluated explicitly using lattice QCD. Early lattice results showed that the disconnected diagrams are relatively small for vector mesons [2] but are relatively large for pseudoscalar (and scalar) mesons. Here we use more precise methods to determine the size of the disconnected diagrams for vector mesons and we discuss the resulting phenomenology.

We describe the vector mesons in a quark model basis for the case of degenerate  $u$  and  $d$  quarks. In the flavour singlet sector, we then have contributions to the mass matrix with quark model content  $(u\bar{u} + d\bar{d})/\sqrt{2}$  and  $s\bar{s}$  (which we label as  $nn$  and  $ss$  respectively):

$$\begin{pmatrix} m_{nn} + 2x_{nn} & \sqrt{2}x_{ns} \\ \sqrt{2}x_{ns} & m_{ss} + x_{ss} \end{pmatrix}. \quad (1)$$

Here  $m$  corresponds to the mass of the flavour non-singlet eigenstate and is the contribution to the mass coming from connected fermion diagrams while  $x$  corresponds to the contribution from disconnected fermion diagrams. Thus  $m_{nn}$  is the  $\rho$  mass. Because of mixing, as will be discussed,  $m_{ss}$  does not correspond exactly to any specific meson. Since the  $K^*$  meson has no disconnected contribution, one approximation is to use the assumption that the connected contribution to the meson mass is linear in the underlying quark masses. Then  $m_{ss} = 2m_{ns} - m_{nn}$ , that is  $2m_{K^*} - m_{\rho}$ , leading to  $m_{ss} = 1.012$  GeV.

The mixing between the  $nn$  and  $ss$  flavour singlet channels must produce the experimental  $\omega(782)$  and  $\phi(1020)$ . We can express the mass eigenstates as

$$m_{nn} + 2x_{nn} - \delta; \quad m_{ss} + x_{ss} + \delta \quad (2)$$

where  $\delta = 2x_{ns}^2/(m_{ss} + x_{ss} - m_{nn} - 2x_{nn})$  to a good approximation for the relevant parameter values. The  $\delta$  term arising from mixing will prove to be small (around 1 MeV mass shift) so that one can estimate the  $\omega$ - $\rho$  mass difference as  $2x_{nn}$  and the upward shift of the  $\phi$  mass due to disconnected diagrams as  $x_{ss}$ . Even though the  $\omega$  -  $\phi$  mixing induces rather small mass shifts, the amplitude mixing can have significant effects. For instance the physical  $\phi$  meson will have a relative amplitude of  $\bar{n}n$  quarks (compared to  $\bar{s}s$ ; this ratio is  $\tan \delta$  where  $\delta$  is the  $\omega$  -  $\phi$  mixing angle) of  $\sqrt{2}x_{ns}/(m_{ss} + x_{ss} - m_{nn} - 2x_{nn})$  which will be of order a few percent and can have an important consequence in  $\phi$  decays to non-strange final states and  $\omega$  production from strange initial states.

The contributions  $x$  from disconnected diagrams will depend on the quark mass. For pseudoscalar mesons, the  $x$  values are rather constant at small quark masses [3] and decrease slowly with increasing quark mass [4]. Something similar would be expected for the vector mesons. One simple phenomenological ansatz would be to assume all  $x$ -values were the same. Then the  $\omega$ - $\rho$  mass difference ( $2x_{nn} = 7.2$  MeV experimentally) should be approximately twice the  $\phi$  mass shift ( $x_{ss}$ ) although with the above model for  $m_{ss}$  this is 7 MeV which does not agree. Such quantitative comparisons are not to be trusted for several reasons: (i) the  $\rho$  meson is so wide (circa 150 MeV) that the impact of its decay on its mass value must introduce an uncertainty of a few MeV at least (ii) the model to estimate the mass shift of the ‘connected’  $\phi$  (meson mass linear in valence quark content) is also imprecise (for example, a meson mass-squared linear in valence quark content gives 5 MeV instead) and (iii) the underlying assumption that the disconnected contributions ( $x$ ) are independent of mass may be at fault. To clarify these ideas, a direct evaluation from QCD is necessary.

In this paper, we study lattice QCD in the unitary sector with  $N_f = 2$  degenerate light quarks. This enables us to extract estimates for the  $\omega$ - $\rho$  mass difference. We can also explore the (sea)quark mass dependence of  $x_{nn}$  which can help to understand the value of  $x_{ss}$  needed to determine the disconnected contribution to the  $\phi$  meson.

There is considerable interest in building reliable models of the quark mass dependence of the  $\rho$  meson. We show that such models inevitably have consequences for the  $\omega - \rho$  mass difference. We compare these predictions with our lattice results.

We also explore effects arising in QCD from the  $u$ - $d$  quark mass difference. This causes a violation of isospin and a mixing between  $\omega$  and  $\rho$  mesons. We are able to evaluate this mixing (given the quark mass difference as input) from the lattice and we compare with experiment.

Here we follow the lattice methods used in our study of the flavour singlet pseudoscalar mesons [5]. The disconnected contributions are evaluated using stochastic methods with variance reduction while the connected contributions are evaluated using stochastic time-plane sources with the ‘one end trick’.

Use of the remarkable precision obtainable [3, 6, 5] in evaluating disconnected contributions in maximally-twisted lattice QCD will enable us to obtain a statistically significant signal for the vector mass splitting.

## 2 Twisted mass lattice QCD and neutral particles

In quenched or partially-quenched lattice QCD, the disconnected contribution to the flavour singlet meson does not combine properly with the connected contri-

Ensemble	$L^3 \times T$	$\beta$	$a\mu_q$	$\kappa$	$r_0/a$
$B_1$	$24^3 \times 48$	3.9	0.0040	0.160856	5.22(2)
$B_2$			0.0064		
$B_3$			0.0085		
$B_6$	$32^3 \times 64$	3.9	0.0040	0.160856	
$C_1$	$32^3 \times 64$	4.05	0.003	0.157010	6.61(3)
$C_2$			0.006		

**Table 1:** Summary of ensembles produced by the ETM collaboration used in this work. We give the lattice volume  $L^3 \times T$  and the values of the inverse coupling  $\beta$ , the twisted mass parameter  $a\mu_q$ , the hopping parameter  $\kappa = (2am_0 + 8)^{-1}$  and the Sommer parameter  $r_0/a$  in the chiral limit from ref. [11, 10]. The data sets cover 5000 equilibrated trajectories (10000 for  $B_1$ ).

bution to give a physical state. To avoid this problem, it is mandatory to study flavour singlet states in full QCD - with sea quarks having the same properties as valence quarks. Then the spectrum of flavour singlet states is well defined and can be extracted from the  $t$ -dependence of the full correlator. Here we focus on the case where there are two degenerate light quarks (called  $N_f = 2$ ) which is a consistent theory in which to study the flavour singlet mesons. We use the twisted mass lattice formalism [7, 8], for a recent review, see ref. [9].

The results presented in this paper are based on gauge configurations as produced by the European Twisted Mass collaboration (ETMC). The details of the ensembles are described in ref. [10]. In particular, we concentrated for this paper on the ensembles labelled  $B_1, B_2, B_3, B_6$  and  $C_1$  and  $C_2$ . We have compiled the details for those ensembles in table 1. The  $B$ -ensembles correspond to a value of the lattice spacing of about  $a \sim 0.09$  fm and the  $C$ -ensembles to  $a \sim 0.07$  fm. The spatial lattice size is of about  $L \sim 2.2$  fm for all ensembles used here, apart from  $B_6$ , which has identical parameters to  $B_1$  but  $L \sim 2.7$  fm. The corresponding pseudoscalar mass is in the range 300-440 MeV.

The twisted mass formalism at maximal twist is order  $a$  improved and allows access to light pseudoscalar mesons [11]. There is one complication, however, namely that the twisted mass lattice formalism breaks flavour and parity symmetries at finite values of the lattice spacing  $a$ . These symmetries are restored in the continuum limit and the theory is well defined (so providing a valid regularisation) at finite lattice spacing. One consequence of this flavour-breaking is that charged and neutral non-singlet mesons can have a mass splitting (of order  $a^2$ ). Moreover, the neutral non-singlet mesons have (order  $a^2$ ) contributions from disconnected diagrams [12, 11]. Note that the order  $a^2$  splitting between  $\rho^+$  and  $\rho^0$  was found to be compatible with zero [3].

In the case of twisted mass fermions, the bilinear operators appropriate to create the  $\omega$  state are  $O_i^V = \bar{\psi}\gamma_i\psi$  and  $O_i^T = \bar{\psi}\gamma_i\gamma_4\psi$  which on transformation into the twisted basis (used in lattice evaluation) will become  $\bar{\chi}\gamma_i\chi$  and  $\bar{\chi}\gamma_i\gamma_4\gamma_5\tau_3\chi$ ,

respectively, where  $\tau_3$  acts in the ( $u$ ,  $d$ ) flavour space. This latter case amounts to evaluating, in the lattice basis, the difference of the disconnected loop between  $u$  and  $d$  quarks. This enables a very efficient variance reduction technique [3, 6, 5] to be used to evaluate the relevant disconnected diagram for the case of the  $O^T$  operator. Here we follow in detail the methods to evaluate the disconnected ( $D$ ) and connected ( $C$ ) meson correlators described in ref [5]. Some discussion of the connected correlators for vector mesons has already appeared [13, 14] and a fuller study is in preparation [15].

The connected meson correlator describes the flavour non-singlet meson ( $\rho$ ), while the combined correlator describes the flavour singlet ( $\omega$ ). Assuming sufficiently large  $t$ -separation so that the ground states dominate, then we have (for  $N_f = 2$ )

$$C(t) = c \exp(-m(\rho)t); \quad C(t) - 2D(t) = d \exp(-m(\omega)t) \quad (3)$$

Hence

$$2D(t)/C(t) = -\frac{d}{c} \exp(-\Delta t) + 1 \quad (4)$$

where  $\Delta = m(\omega) - m(\rho)$ . Moreover, if  $\Delta$  is small, as we shall find, then

$$2D(t)/C(t) = \frac{d}{c} \Delta t + (1 - \frac{d}{c}) \quad (5)$$

Since the difference between  $\rho$  and  $\omega$  is so small, one would also expect the creation amplitudes to be equal so that  $d \approx c$ . Then keeping the first order in the mass splitting, this leads to the simple result that  $2D(t)/C(t) = \Delta t + \mathcal{O}(\Delta)$  which will be a good approximation provided  $\Delta t \ll 1$ .

In twisted mass QCD, there is an order  $a^2$  contribution to the  $\rho^0$  meson propagation arising from disconnected diagrams. This has been studied previously [3] using the operator  $O^V$  which enables the variance reduction method to give precise results in this case. No statistically significant contribution was found. For our present purposes, however, we wish to focus on the disconnected contribution to the  $\omega$  meson compared to its connected contribution which is in turn equal to the connected contribution of the  $\rho^0$  propagation. So we compare the  $\omega$  propagation with that of the connected contribution ( $C$ ) for the  $\rho^0$  meson.

We present some results for this ratio  $2D/C$  in fig. 1. We have evaluated this for local meson operators (L) and non-local (fuzzed) meson sources (F).

In order to interpret this signal we evaluate the effective mass from the connected component which is displayed in fig 2. This shows that the ground state dominates in this case for  $t/a > 5$  for the LF and FF cases. This allows us to interpret the data in fig. 1 as being dominated by the ground state for that  $t$ -region, so that one can determine the mass splitting from the slope as described above.

We fit the behaviour of  $2D/C$  as a straight line (eq. 5) in the range of  $t/a$  from 5 to 12 (6 to 12 for the LL results) for  $\beta = 3.9$  and 6 to 16 (7 to 15 for

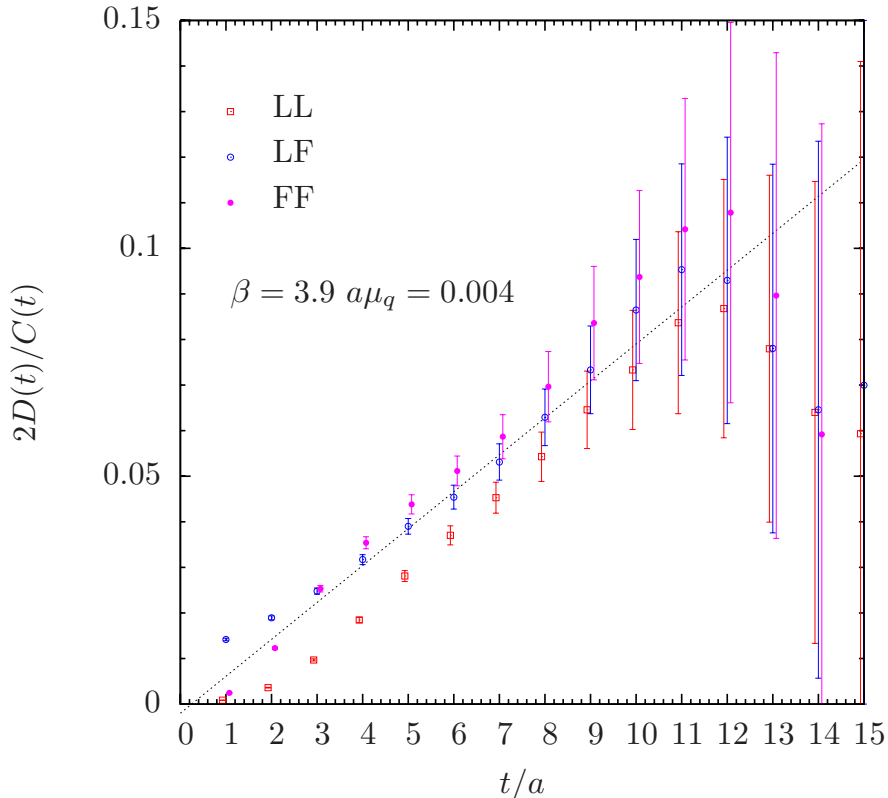


**Figure 1:** Ratio of disconnected to connected contribution to neutral vector meson (created by  $O^T$ ) versus  $t$ . Results are from ensemble  $B_1$  ( $L = 24$ ) with  $a\mu_q = 0.004$ . The ratio is given for cases with local operator at source and sink (LL) and for cases when one or both operator is non-local (fuzzed F). The line represents the fit to the LF data in the  $t/a$ -range 5 to 12.

LL) for  $\beta = 4.05$ . The  $\chi^2$  of these fits is acceptable. We take the average of the slope from the LF and FF fits and we determine an error for the slope  $a\Delta$  from combining the range of values found (including the LL case). The intercepts are very close to zero, so the impact of the factor  $d/c$  on the determination of  $\Delta$  in eq. 5 is negligible. We find that the results from two different volumes (spatial extent  $L=24$  and  $32$  at  $\mu_q = 0.004$ ) are consistent with each other.

In order to compare the results from different lattice spacings, we plot them using the  $r_0/a$ -values given in table 1 to convert our results to GeV units using  $r_0 = 0.454(7)\text{fm}$  obtained [11] from the ETMC evaluation of  $f_\pi$ . We show the  $\omega$ - $\rho$  mass splitting in fig. 3 and we see that our results at different lattice spacings are consistent with each other.

Extrapolation to the physical limit (for  $u$  and  $d$  quarks) gives  $m(\omega) - m(\rho) = 27(5)$  MeV assuming a linear dependence. Since there is limited evidence for the form of the extrapolation, we assign a error which covers the possibility of a constant extrapolation (namely  $27(10)$  MeV).

This may be compared with the experimental splitting [1] of 7.2 MeV. In our

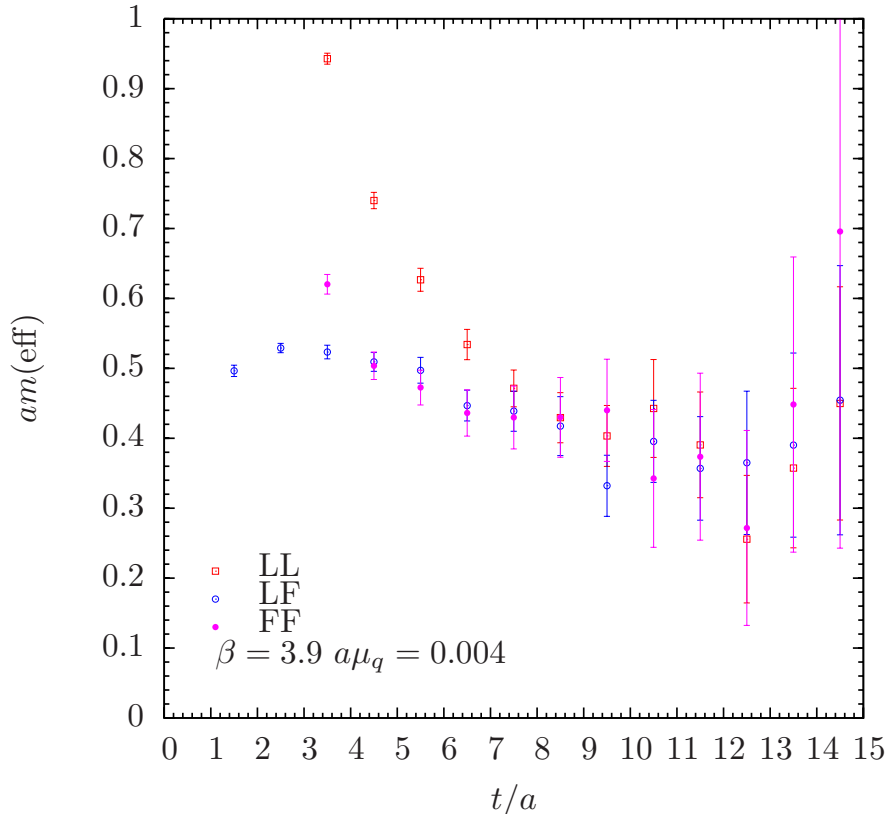


**Figure 2:** The effective mass (in lattice units) of the connected contribution to the neutral vector meson (created by  $O^T$ ) versus  $t$ . Results are from ensemble  $B_6$  ( $L = 32$ ) with  $a\mu_q = 0.004$  and  $r_0/a = 5.22$ . The result is given for cases with local operator at source and sink (LL) and for cases when one or both operator is non-local (fuzzed F).

QCD study, we do not include electromagnetic effects or effects arising from the  $u$ - $d$  quark mass difference. These effects are estimated [16] to be of the order of a few MeV. Furthermore, the definition of the  $\rho$  mass is uncertain to a similar extent, because it is such a wide resonance. Hence precise agreement between the observed  $\omega$ - $\rho$  mass difference and that found from lattice QCD is not to be expected.

The quark mass dependence of vector meson masses is of considerable interest, especially in the lattice community. Next we discuss models which may be compared with our results.

### 3 Models for vector meson masses

The disconnected quark diagram that contributes to the  $\omega$ - $\rho$  mass difference can be used to inform models of the mass-dependence of the vector meson masses on the underlying quark mass. Such models contain contributions from two-particle

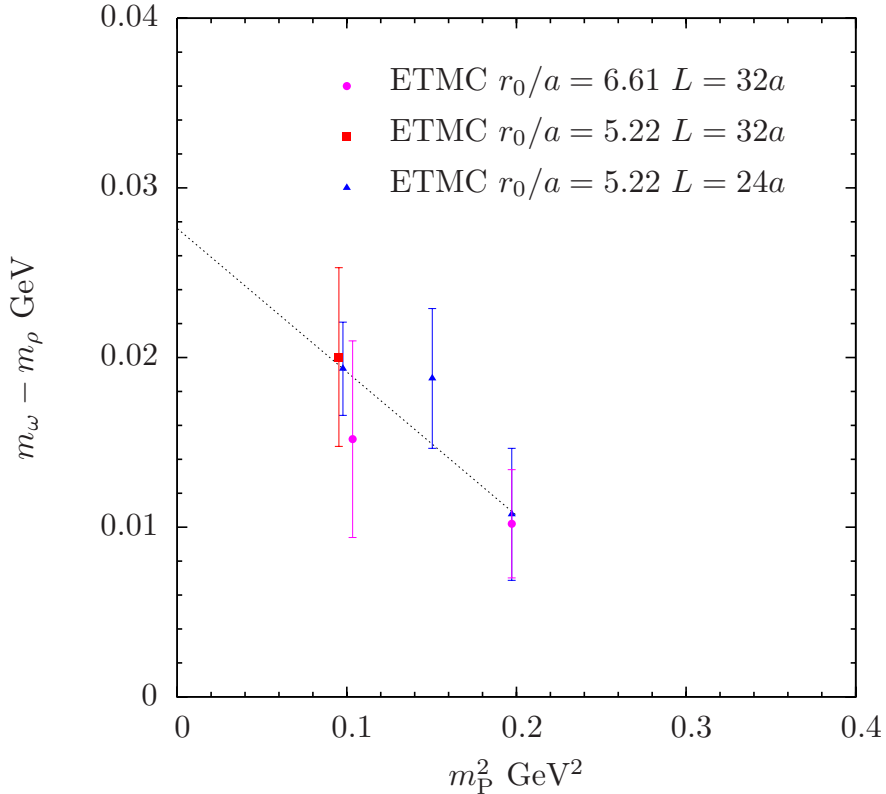


**Figure 3:** The  $\omega$ – $\rho$  mass difference versus the quark mass given by  $m_P^2$ . A linear extrapolation is plotted. The lattice spacing is  $a$  and the spatial extent of the lattice is  $L$ .

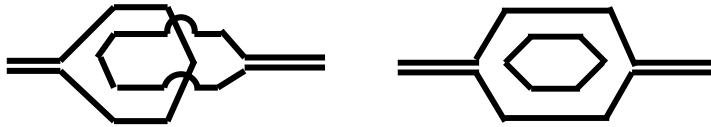


**Figure 4:** Disconnected and connected two-particle intermediate states.

intermediate states evaluated in some effective theory. One contribution to the  $\omega$ – $\rho$  mass difference comes from such two particle contributions to the self energy. This gives an excellent way to check on these effective Lagrangian models for the  $\rho$  mass versus  $m_\pi$ . Here we retain the physical meson names ( $\rho$ ,  $\omega$ ,  $\pi$ ) to describe mesons with these quantum numbers as the light quark mass is varied.

One way to visualise this contribution to disconnected diagrams from two-particle intermediate states is illustrated by the two quark diagrams describing disconnected and connected quark line contributions in fig. 4.

The two-body contributions (having non-analytic behaviour with  $m_\pi$ ) that are usually considered are the pseudoscalar-pseudoscalar (PP) and vector-pseudoscalar (VP) intermediate states. Here we tabulate the relative contributions to  $\rho$  and  $\omega$  mesons:



V	PP	VP
$\rho$ :	$\pi\pi$	$\omega\pi$ ( $1g^2$ )
$\omega$ :	-	$\rho\pi$ ( $3g^2$ )

The notation for the VP case indicates that  $\omega \rightarrow \rho\pi$  has 3 terms ( $\rho^0\pi^0$ ,  $\rho^+\pi^-$ ,  $\rho^-\pi^+$ ) whereas  $\rho \rightarrow \omega\pi$  has just one ( $\omega^0\pi^0$  but with the same coupling). Thus the contributions from these intermediate states to the  $\omega - \rho$  mass difference are  $VP(2g^2) - PP$  while the  $\rho$  mass has  $VP(1g^2) + PP$ . This exemplifies the link between models for the quark mass dependence of the  $\rho$  meson and models for the  $\omega - \rho$  mass difference.

We now discuss some models proposed and focus on their implications for the  $\omega - \rho$  mass difference. We first consider the VP intermediate state. The behaviour of this contribution versus quark mass is as  $m_\pi^3$  and estimates of the contribution (without using any form factor) to the  $\rho$  mass at the physical pion mass are 3.4 MeV [16] and 5 MeV [17]. The strong dependence on  $m_\pi$  implies that, in these models, the VP contribution for a pion mass around 300 MeV will be much bigger: for the  $\omega - \rho$  mass difference they obtain values of -70 MeV [16] and -30 MeV [17] using a form factor cutoff. This large value obtained without cutoff is quoted as ‘not to be taken too seriously’ by ref. [16]. For more discussion of regulators which may improve the convergence, see also ref. [18]. In our opinion, the evaluation of the VP intermediate state is delicate since as the quark mass decreases, the V and VP states become nearly degenerate. In this circumstance, one needs to take account of the width of the  $\rho$  meson which could modify the expressions significantly.

The PP intermediate state (i.e.  $\pi\pi$  contribution to the  $\rho$ ) has a non-analytic component behaving as  $m_\pi^4 \log(m_\pi)$ . One approach [17] uses the relativistic matrix element but introduces a form factor to emphasize the kinematic region where the model should be more reliable. Fitting to lattice data, they obtain a contribution to the  $\rho$  mass of -35 MeV for the physical pion mass and -40 MeV for pion masses around 300 MeV. These values imply a contribution to the  $\omega - \rho$  mass difference of 40 MeV for pion masses around 300 MeV.

In summary, models give quite large contributions to the  $\omega - \rho$  mass difference, with the VP intermediate state dominating, and becoming more negative as the quark mass is increased. However the models have an increasingly large contribution at larger masses which needs to be tamed by a cutoff or other method. Our lattice data show a decrease with increasing quark mass, but with numerical values that are much smaller than those typically given by models.

## 4 $\omega - \rho$ mixing

Within QCD when  $m_u \neq m_d$ , isospin is not a good quantum number and there is a mixing matrix element between the  $\omega$  and  $\rho$  mesons. One experimental manifestation of this is the decay  $\omega \rightarrow \pi\pi$  which creates an interference pattern

in the dominant decay  $\rho \rightarrow \pi\pi$  near the  $\omega$  mass. The mixing can be defined from a mass matrix (with basis states  $(\bar{u}\gamma_i u \pm \bar{d}\gamma_i d)/\sqrt{2}$ ):

$$\begin{pmatrix} m_\rho & T_{\omega\rho} \\ T_{\omega\rho} & m_\omega \end{pmatrix}. \quad (6)$$

Phenomenologically [19] the transition matrix element  $T_{\omega\rho} = -3.1(3)$  MeV. Some of the observed effect can come from electromagnetic contributions and these are estimated [16] to contribute between 0.4 and 1.2 MeV. So the QCD contribution would be around -4 MeV.

We can study this contribution on a lattice by considering the cross correlator: create a  $\omega$  meson (using  $(\bar{u}\gamma_i u + \bar{d}\gamma_i d)/\sqrt{2}$ ) and destroy a  $\rho$  meson (using  $(\bar{u}\gamma_i u - \bar{d}\gamma_i d)/\sqrt{2}$ ). This cross correlator will have a connected piece (like  $(C_u - C_d)/2$ ) and a disconnected piece. The disconnected contribution simplifies using the identity  $D_{ud} = D_{du}$  yielding  $(D_{uu} - D_{dd})/2$ . Here  $D_{ud}$  means the correlator between a  $u$ -quark loop at source and a  $d$ -quark loop at sink. Because of the form of the cross-correlator, it may be expressed as a difference between propagation of vector mesons containing quarks of different mass. It may then be related (using techniques similar to those used in ref. [20] and assuming that  $(m_\omega - m_\rho)t \ll 1$  to simplify the expression) to the mass-matrix transition element:

$$T_{\omega\rho} = \left( \frac{dm_\rho}{dm_q} + \frac{dm_\omega}{dm_q} \right) \frac{m_u - m_d}{4} \quad (7)$$

where we have assumed that we may retain the first power of  $m_u - m_d$  only. Here the derivatives are with respect to the degenerate quark mass in an  $N_f = 2$  theory. These derivatives are those that we have access to from our study above.

We can estimate this transition rate phenomenologically, using  $dm_\rho/dm_\pi^2 \approx 1/(2m_\rho)$  (from the  $\phi$ ,  $K^*$  and  $\rho$  masses, see ref. [21]) and  $dm_\omega^2/dm_q = m_\pi^2/\hat{m}_q$  (from lowest order ChPT). Here  $\hat{m}_q$  is the average light quark mass  $(m_u + m_d)/2$ . This gives us

$$T_{\omega\rho} = -\frac{1 - m_u/m_d}{1 + m_u/m_d} \frac{m_\pi^2}{2m_\rho} \quad (8)$$

and with  $m_u/m_d = 0.56$  from lowest order of ChPT [1] we obtain  $T_{\omega\rho} = -3.6$  MeV which is close to the experimentally determined value.

We now discuss evaluation of the above expression in eq. 7 using lattice results from first principles. This involves the quark mass dependence of the  $\rho$  and  $\omega$  masses in an  $N_f = 2$  theory, which we have available. In particular we are able to address the quark mass dependence of the disconnected contribution to the  $\omega$  mass, which has not been studied previously.

Since  $dm_\rho/dm_q + dm_\omega/dm_q = 2dm_\rho/dm_q + d(m_\omega - m_\rho)/dm_q$  we compare these two terms. We can evaluate  $d(m_\omega - m_\rho)/dm_q^2$  as the slope shown in fig. 3.

We obtain a slope  $-0.15(15)/(2m_V)$  where the error encompasses the possibility of a constant behaviour which is not strongly excluded by our lattice results. Compared to the phenomenological estimate that  $dm_\rho/dm_P^2 \approx 1/(2m_V)$ , this value indicates that the contribution of the  $\omega$  meson disconnected diagram to the  $\omega - \rho$  mixing is relatively insignificant (at around 7%) - in agreement with earlier phenomenological estimates [16].

We find that lattice QCD naturally produces effects of the correct size to explain the observed  $\omega$ - $\rho$  mixing.

## 5 Summary

Previous lattice results were very exploratory: for  $N_f = 2$  sea quarks of mass (given by  $(r_0 m_{PS})^2 = 3.7$ ) corresponding to about 1.5 times the strange quark mass, an  $\omega$ - $\rho$  mass difference of 2(3) MeV was obtained [2] with quite strong evidence that the sign of the effect should be positive (the same as found here). A more recent study finds [22], in the chiral limit, an  $\omega$  mass of 790(194) MeV, fixing the scale at the  $\rho$  mass: so a mass difference of 15(194) MeV.

Here we have presented results coming from a well established signal and we are able to address issues such as extrapolation to the continuum limit. We see in fig. 3 that our results are consistent with each other at different lattice spacing and for different lattice spatial volumes. There is evidence for a reduction in the splitting with increasing quark mass. Since there is limited evidence for the form of the extrapolation to the physical point, we assign a error which covers the possibility of a constant extrapolation (namely 27(10) MeV).

This may be compared with the experimental splitting [1] of 7.2 MeV. The experimental result includes electromagnetic effects (estimated to be of order a few MeV) and the definition of the  $\rho$  mass is uncertain to a similar extent, because it is such a wide resonance. Hence precise agreement between the observed  $\omega$ - $\rho$  mass difference and that found from lattice QCD is not to be expected. What we do establish, however, is that there are substantial contributions to the  $\omega$ - $\rho$  mass difference arising within QCD from the disconnected contributions (known phenomenologically as OZI violating contributions). Moreover, these contributions are of the same sign as the experimentally observed difference.

Our study shows that it is possible to extract a signal for the  $\omega - \rho$  mass splitting versus quark mass and that this quantity will be very useful in refining models for vector mesons near the chiral limit. Indeed some existing models give results which are significantly different from those we obtain (especially for the VP intermediate state contribution).

We also showed from first principles that the observed  $\omega$ - $\rho$  mixing arises naturally in QCD with the correct magnitude. We were able to estimate, for the first time, the contribution to this mixing arising from disconnected diagram contributions and we showed that it is relatively unimportant.

It has been suggested that the  $\omega - \rho$  mixing is the mechanism behind charge symmetry breaking in nucleon-nucleon interactions. However there are other competing mechanisms (see Miller et al. [19] for a review) that try to explain charge symmetry breaking. One problem with the proposed mechanism of  $\omega - \rho$  mixing for charge symmetry breaking in the nuclear force is that the momentum dependence of the mixing was hard to constrain. Although we have only evaluated the  $\omega - \rho$  mixing at zero momentum, our techniques can in principle be used to investigate the momentum dependence [23], so our calculation is the first step in determining the mechanism of charge symmetry breaking in the nuclear force from first principles.

Although we have studied QCD with  $N_f = 2$  light degenerate fermions, one can extend the discussion to include the strange quark by assuming that the disconnected contribution is independent of the quark mass, so yielding an estimate of  $x_{ns} \approx x_{nn} = 13(5)$  MeV. This implies that the  $\phi$ - $\omega$  Hamiltonian mixing amplitude given by  $\sqrt{2}x_{ns}$  should be of comparable size. This is in qualitative agreement with phenomenology [16] which finds values of 8 to 14 MeV from an analysis of  $\phi$  decays.

The mixing between the  $\omega$  and  $\phi$  is required to understand  $B$  and  $D_s$  decays with an  $\omega$  or  $\phi$  in the final state [24, 25]. For example Gronau and Rosner [25] predict the branching ratio  $\mathcal{B}(D_s^+ \rightarrow \omega e^+ \nu_e) / \mathcal{B}(D_s^+ \rightarrow \phi e^+ \nu_e)$  in terms of the  $\omega - \phi$  mixing angle. Other mechanisms can contribute to this ratio, such as "weak annihilation", so a first principles calculation of the  $\omega - \phi$  mixing angle is valuable.

In summary, the vector mesons have a rich structure beyond 'ideal mixing' and this rich structure can be evaluated accurately using lattice QCD.

## Acknowledgments

We acknowledge helpful advice from members of the ETM Collaboration and computing resources provided by NW Grid at Liverpool and by HLRN at Berlin.

## References

- [1] Particle Data Group, C. Amsler *et al.*, Phys. Lett. **B667**, 1 (2008).
- [2] UKQCD, C. McNeile, C. Michael and K. J. Sharkey, Phys. Rev. **D65**, 014508 (2002), [hep-lat/0107003].
- [3] ETM, C. Michael and C. Urbach, (2007), [arXiv:0709.4564 [hep-lat]].
- [4] UKQCD, C. McNeile and C. Michael, Phys. Lett. **B491**, 123 (2000), [hep-lat/0006020].
- [5] ETM, K. Jansen, C. Michael and C. Urbach, 0804.3871.

- [6] ETM, P. Boucaud *et al.*, *Comput. Phys. Commun.* **179**, 695 (2008), [0803.0224].
- [7] Alpha, R. Frezzotti, P. A. Grassi, S. Sint and P. Weisz, *JHEP* **08**, 058 (2001), [hep-lat/0101001].
- [8] R. Frezzotti and G. C. Rossi, *JHEP* **08**, 007 (2004), [hep-lat/0306014].
- [9] A. Shindler, *Phys. Rept.* **461**, 37 (2008), [0707.4093].
- [10] ETM, C. Urbach, arXiv:0710.1517 [hep-lat].
- [11] ETM, P. Boucaud *et al.*, *Phys. Lett.* **B650**, 304 (2007), [hep-lat/0701012].
- [12] XLF, K. Jansen *et al.*, *Phys. Lett.* **B624**, 334 (2005), [hep-lat/0507032].
- [13] ETM, P. Dimopoulos, C. McNeile, C. Michael, S. Simula and C. Urbach, 0810.1220.
- [14] P. Dimopoulos *et al.*, *PoS LATTICE2008*, 271 (2008), [0810.2443].
- [15] ETMC, in preparation .
- [16] J. Bijnens and P. Gosdzinsky, *Phys. Lett.* **B388**, 203 (1996), [hep-ph/9607462].
- [17] D. B. Leinweber, A. W. Thomas, K. Tsushima and S. V. Wright, *Phys. Rev.* **D64**, 094502 (2001), [hep-lat/0104013].
- [18] P. C. Bruns and U.-G. Meissner, *Eur. Phys. J.* **C40**, 97 (2005), [hep-ph/0411223].
- [19] G. A. Miller, A. K. Opper and E. J. Stephenson, *Ann. Rev. Nucl. Part. Sci.* **56**, 253 (2006), [nucl-ex/0602021].
- [20] UKQCD, M. Foster and C. Michael, *Phys. Rev.* **D59**, 074503 (1999), [hep-lat/9810021].
- [21] UKQCD, P. Lacock and C. Michael, *Phys. Rev.* **D52**, 5213 (1995), [hep-lat/9506009].
- [22] K. Hashimoto and T. Izubuchi, *Prog. Theor. Phys.* **119**, 599 (2008), [0803.0186].
- [23] UKQCD, C. McNeile, C. Michael and P. Pennanen, *Phys. Rev.* **D65**, 094505 (2002), [hep-lat/0201006].
- [24] M. Gronau and J. L. Rosner, *Phys. Lett.* **B666**, 185 (2008), [0806.3584].
- [25] M. Gronau and J. L. Rosner, 0902.1363.